



ELSEVIER

15 December 1998

OPTICS
COMMUNICATIONS

Optics Communications 158 (1998) 273–286

Full length article

Generation of squeezed states and twin beams via non-degenerate four-wave mixing in a Λ system

M.S. Shahriar^{a,*}, P.R. Hemmer^b

^a *Research Laboratory of Electronics, Massachusetts Institute of Technology, Cambridge, MA 02139, USA*

^b *Air Force Research Laboratory, Hanscom Air Force Base, Bedford, MA 01731, USA*

Received 23 September 1998; accepted 29 September 1998

Abstract

We show that non-degenerate four-wave mixing in a Λ system yields strong suppression of quantum phase noise when the probe and conjugate beams are monitored via balanced homodyne detection. Unlike previous calculations performed on similar system, we include situations where the pump beams become resonant with the corresponding two-level transitions. As a result, we find conditions wherein strong squeezing can be achieved with relatively low pump powers. Furthermore, we show explicitly, via numerical integration, that the probe and the conjugate beams, each starting from the vacuum, are twin beams, containing matching number of photons. The low-power, high gain phase conjugation observed experimentally by us in rubidium vapor under similar conditions indicate the feasibility of realizing a spatially broad band source of squeezed light, with applications to fast detection of faint images, as well as to high-density optical interconnects. © 1998 Published by Elsevier Science B.V. All rights reserved.

PACS: 42.50.-p; 42.50.Lc; 42.50.Dv; 32.80.-t

Keywords: Λ system; Non-degenerate four-wave mixing; Quantum phase noise

1. Introduction

Squeezed states of light are special quantum mechanical states of the electromagnetic field where the shot noise (resulting from the Heisenberg uncertainty principle) for a particular phase of the field is reduced at the expense of increasing the shot noise at the orthogonal (quadrature) phase. If this field is detected at this particular phase only, the signal to noise ratio is much less than the shot noise. For physical understanding, this process can be thought of as sending the light through a ‘shutter’ which is preferentially opened only during a small part of the optical oscillation period. From a quantum optics point of view, the squeezed states are formed by creating an entanglement among two photons. As such, there is no classical model for such a state. Squeezed states were first observed at AT&T by Slusher et al. [1] in a two-level system of sodium atoms. Many groups have since observed squeezing of quantum noise (for example, Refs. [2,3]).

Initially, the predominant point of interest in squeezed states was centered around the possibility of using squeezed light to enhance the sensitivity of optical interferometers, especially for demanding applications such as detection of gravitational waves [4] and observation of the General Relativistic frame-dragging via the Lense–Thirring rotation [5]. The pioneering

* Corresponding author. E-mail: smshari@mit.edu

experiment by Xiao et al. [6] where sub-shot-noise interferometry was observed provided a strong encouragement for this pursuit. However, recently it has become clear that in practical situations squeezed states are not expected to play a significant role in ultra-precision interferometry, for two reasons. First, the degree of squeezing observed has remained limited, owing to imperfect quantum efficiency of detectors. Second, the interferometers that yield the best sensitivities are not easily amenable to improvements via use of squeezed light. For example, the best Sagnac interferometer for precision rotation sensing uses a He–Ne ring laser, where the properties of the active medium is critically important for the optimum performance [7]. To date, nobody has been able to show how this interferometer can be improved by using squeezed light. As such, the interest in squeezed states for precision rotation sensing has dwindled considerably.

Over the last couple of years, efforts have been underway to identify other areas where squeezed light might be useful. One exciting development in this regard is the realization that, by extending squeezing into spatial domains, it might be possible to detect faint images, with sub-shot-noise sensitivity [8]. One intriguing application of such a process is in the area of optical interconnects. The recent developments in the area of optical memory using spectral hole-burning media has led to the possibility of developing an optical DRAM with a capacity of more than 100 Gbyte within a few years [9–11]. However, one key constraint in using such a memory most effectively is the lack of an interconnect that can detect 10^8 or more bits simultaneously. Consider, for example, the detector array in such a processor. For a signal-to-noise ratio of 10 (the current standard minimum for data fidelity), each detector must absorb about 100 photons within the detection period. Given that the chip size must be limited by the optical geometry, the heat generation becomes prohibitive for a processor with more than 10^6 bits. Even with a modest degree (e.g., 10 dB) of squeezing, the number of photons per detector can be reduced by a factor of 10, so that the number of elements in the two-dimensional array can be increased by a factor of 100.

In order to achieve this objective of sub-shot-noise detection of faint images, what is needed is a mechanism that will produce spatially broad band squeezing, with a large bandwidth. However, to date, the methods that have yielded the best squeezing uses a three wave mixing process, typically via optical parametric amplification in a KTP crystal (for example, Refs. [2,3]). Such a process is quite limited in spatial bandwidth, due to the constraints of χ_2 -type phase matching. What is necessary is a four-wave mixing process, obeying a χ_3 -type phase matching, that yields strong squeezing.

As proposed originally by Yuen and Shapiro [12], one of the best medium displaying such non-linearity is a two-level atom driven near resonance. However, as realized by Slusher et al. [1], in order to avoid the deleterious effects of noise due to absorption (which in turn is tied to spontaneous emission), it is necessary to drive such a system far off-resonance in order to observe squeezing. The amount of pump power available limits the degree of detuning, thus limiting the degree of squeezing achievable to very low values (less than 3 dB). This problem is also at the heart of the limitation of such a system as a phase conjugator [13]. In addition, the high pump powers and high atomic densities needed for squeezing in two-level systems leads to severe image distortions due to inhomogeneous absorption as well as Kerr-type non-linearities.

We have found that when a folded three-level (Λ) system, instead of a two-level system, is used to perform squeezing via four-wave mixing, these concerns are largely alleviated. Briefly, we predict that very strong squeezing can be achieved at typical powers available experimentally. This is because the optical non-linearity responsible for squeezing is generated by a two-photon transition that couples the two low-lying states of the Λ system. The gratings responsible for four-wave mixing are formed as the atoms get optically pumped into the spatially varying dark state, via coherent population trapping (CPT) [14,15]. As such, a very strong grating can be produced without having to saturate the individual two-level transitions along each leg. In a series of recent experiments, we have used this fact to demonstrate very efficient phase conjugators in vapors of sodium and rubidium [16,17]. Moreover, the two photon transition tends to push the system into a transparent state (the so-called dark state), so that the images can propagate without distortion. We have already observed such distortion free, diffraction limited amplification and phase conjugation of a probe in such a system of sodium atomic vapor [18].

In this paper, we study the prospect of using this system for squeezing of quantum noise. Specifically, we show that non-degenerate four-wave mixing in a Λ system yields strong suppression of quantum phase noise when the probe and conjugate beams are monitored via balanced homodyne detection. We include situations where the pump beams become resonant with the corresponding two-level transitions. As a result, we find conditions wherein strong squeezing can be achieved with relatively low pump powers. Furthermore, we show explicitly, via numerical integration, that the probe and the conjugate beams, each starting from the vacuum, are twin beams, containing matching number of photons. The low-power, high gain phase conjugation observed experimentally by us in rubidium vapor [16] under similar conditions indicate the feasibility of realizing a spatially broad band source of squeezed light, with applications to fast detection of faint images, as well as to high-density optical interconnects.

Previously, several authors have studied generation of squeezed light using a Λ transition. For example, Reid et al. [19] considered a scheme where the two legs of the Λ transitions differ in frequency, and the pump and probe beams are degenerate. The calculation is performed in the limit of a large detuning with respect to the two-level transitions, so that the excited level could be eliminated adiabatically. This approximation precluded the conditions under which squeezing can be achieved near the two-level resonances, which requires a low pump intensity. Razmi and Eberly [20] considered squeezing in a Λ system under degenerate excitation, in the limit where the energy difference between the two low-lying levels vanishes.

Unlike the present work, the authors consider a situation where atoms are pumped into the two lower levels. Furthermore, this work does not take into account the role of spontaneous emission in determining the degree of squeezing achievable. Bogolubov et al. [21] considered non-degenerate four-wave mixing for generation of squeezed light, using a ladder type three-level system. In this work, squeezing results from collective effects; in order to achieve 10 dB of squeezing, it is necessary to have 10^3 atoms in a volume much smaller than λ^3 , where λ is the smallest of the wavelengths of light involved. If we use the customary model that the atoms have to be localized to a length scale at least a factor of 10 less than λ in order to see strong collective effects, this condition corresponds to a density of 10^{18} cm^{-3} for a laser wavelength of $1 \mu\text{m}$. In contrast, for the system presented in this paper, the same degree of squeezing is predicted for a density of only $1.5 \times 10^7 \text{ cm}^{-3}$. As such, the work presented here differs significantly from the cases considered previously; in particular, we consider a situation that corresponds to an excitation scheme and laser intensity levels easily realizable experimentally, as evidenced by comparing the parameters with those used for our recent four-wave mixing experiments in rubidium vapor [16], while taking into account the potentially deleterious effects of spontaneous emission.

2. Theory of non-degenerate four-wave mixing in a three-level (Λ) system

2.1. Basic approach

Fig. 1 illustrates schematically the configuration for non-degenerate four-wave mixing in a Λ system. Fig. 1a shows the energy levels and transitions involved. Briefly, the levels $|a\rangle$ and $|b\rangle$ are long-lived, while the level $|e\rangle$ decays at the rate of Γ , equally to levels $|a\rangle$ and $|b\rangle$. The forward pump (F) and the conjugate (C) interact along the $a \leftrightarrow e$ transition, while the backward pump (B) and the signal beams (S) interact along the $b \leftrightarrow e$ transition. The forward and signal beams write a grating in the coherence between states $|a\rangle$ and $|b\rangle$. The backward beam scatters off this grating, creating the conjugate beam, which propagates counter to the signal beam. Fig. 1b shows the physical geometry of the wave mixing process. Since this process obeys spatially broadband phase-matching, the signal beam S can have large angular spreads around the mean angle, which in turn means that S can carry a high-resolution image. The conjugate beam, C, will carry the phase conjugate

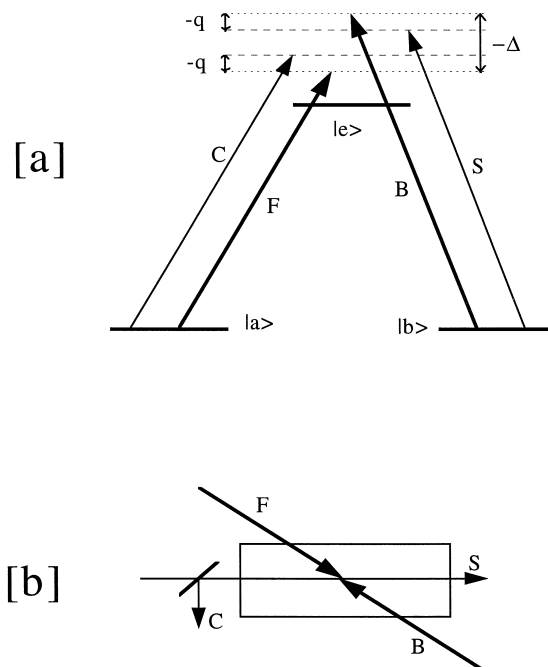


Fig. 1. Schematic illustration of the levels and geometry used for non-degenerate four-wave mixing in a folded three-level system.

Table 1
Definitions of symbols in Eq. (1)

Symbol	Name	Definition/Comment
ε_i	Atomic level energy	$i = a, b, \text{ or } e$
ω_1	Leg 1 transition frequency	$\omega_1 \equiv (\varepsilon_e - \varepsilon_a)/\hbar$
ω_2	Leg 2 transition frequency	$\omega_2 \equiv (\varepsilon_e - \varepsilon_b)/\hbar$
ν_i	Frequency of i th mode	$i = 1, 2, 3, \text{ or } 4$
$-2V_k$	Rabi frequencies of pumps	$k = 1, 2$
g_q	Vacuum rabi frequencies of side-modes	$q = 3, 4$
a_q	Lowering operator for side-modes	$q = 3, 4$
Ω_s	Frequency of vacuum modes	$s \in \{-\infty, \infty\}$, but $s \neq 1, 2, 3, 4$
σ_{1+}	Leg 1 raising operator	$\sigma_{1+} \equiv e\rangle\langle a \equiv \sigma_{1-}^+$
σ_{2+}	Leg 2 raising operator	$\sigma_{2+} \equiv e\rangle\langle b \equiv \sigma_{2-}^+$

replica of the image carried by S. The amplified signal, S', exits in the forward direction, while the conjugate coming out in the backward direction. C can be separated from S by using a beam splitter, as shown.

In order to calculate the degree of squeezing achievable in this system, we use the formalism developed by Holm and Sargent [22] Briefly, we consider the pump beams to be classical fields, and the side-mode (probe and conjugate) fields to be fully quantized. The complete Hamiltonian for the system can be written as:

$$H \equiv H_0 + H_I \tag{1}$$

where H_0 is the energy of the atom interacting with the vacuum modes as well as the classical pumps, and H_I is the energy of interaction between the atom and the side-mode fields. The various contributions to H_0 can be categorized as

$$H_0 = H_A + H_{AP} + H_{AR} + H_R \tag{1.1}$$

where H_A is the energy of the atom, H_{AP} is the energy of interaction between the atom and the classical pump fields, H_{AR} is the energy of interaction between the atom and the reservoir (vacuum) modes, and H_R is the energy of the reservoir modes. These, in turn, are given by:

$$H_A \equiv \hbar \omega_1 \sigma_{1+} \sigma_{1-} + \hbar \omega_2 \sigma_{2+} \sigma_{2-}, \tag{1.1.1}$$

$$H_{AP} \equiv \hbar [V_1 \sigma_{1+} \exp(-i\nu_1 t) + \text{adj.}] + \hbar [V_2 \sigma_{2+} \exp(-i\nu_2 t) + \text{adj.}], \tag{1.1.2}$$

$$H_{AR} \equiv \hbar \sum_{s=-\infty (s \neq 1,2,3,4)}^{\infty} [g_s a_s (\sigma_{1+} + \sigma_{2+}) + \text{adj.}], \tag{1.1.3}$$

$$H_R \equiv \hbar \sum_{s=-\infty (s \neq 1,2,3,4)}^{\infty} \Omega_s a_s^+ a_s. \tag{1.1.4}$$

Similarly, the energy of interaction between the atom and the side-modes is given by:

$$H_I \equiv \hbar (g_3 a_3 \sigma_{1+} + \text{adj.}) + \hbar (g_4 a_4 \sigma_{2+} + \text{adj.}) \tag{1.2}$$

The various parameters here are defined in Table 1.

2.2. Langevin–Bloch equations for the pump–atom interaction

Consider first the response of the atoms to the two pump fields and the vacuum bath. It is convenient to use an interaction picture by defining the operators:

$$S_{1+} \equiv \sigma_{1+} \exp(-i\nu_1 t) \equiv S_{1-}^+ \tag{2.1}$$

$$S_{2+} \equiv \sigma_{2+} \exp(-i\nu_2 t) \equiv S_{2-}^+ \tag{2.2}$$

Using the Markoff approximation, we write the Langevin–Bloch equation as:

$$\frac{\partial}{\partial t} \vec{A}(t) = \vec{B} \cdot \vec{A}(t) + \vec{C} + \vec{f}(t) \tag{3.1}$$

Here, $\vec{A}(t)$ is an eight-element (rotating wave) vector representing the state of the atom, \vec{C} is a constant representing the invariance of the sum of atomic populations, $\vec{f}(t)$ is the Langevin force, and \vec{B} is the time propagation operator. Explicitly,

$$\vec{A}(t) \equiv \begin{bmatrix} S_{1+} \\ S_{1-} \\ S_{2+} \\ S_{2-} \\ S_{3+} \\ S_{3-} \\ S_{1Z} \\ S_{2Z} \end{bmatrix} \equiv \begin{bmatrix} \sigma_{1+} \exp(-i\nu_1 t) \\ S_{1+}^+ \\ \sigma_{2+} \exp(-i\nu_2 t) \\ S_{2+}^+ \\ S_{2-} - S_{1+} \\ S_{3+}^+ \\ \frac{1}{2}(S_{1+}S_{1-} - S_{1-}S_{1+}) \\ \frac{1}{2}(S_{2+}S_{2-} - S_{2-}S_{2+}) \end{bmatrix}, \quad \vec{C} \equiv \begin{bmatrix} 0 \\ 0 \\ 0 \\ 0 \\ 0 \\ 0 \\ -\Gamma/4 \\ -\Gamma/4 \end{bmatrix}, \quad \vec{f} \equiv \begin{bmatrix} f_1 \\ f_2 \\ f_3 \\ f_4 \\ f_5 \\ f_6 \\ f_7 \\ f_8 \end{bmatrix} \quad (3.2)$$

$$\vec{B} \equiv \begin{bmatrix} -i(\delta + \Delta/2) - \Gamma/2 & 0 & 0 & 0 & iV_2^* & 0 & -i2V_1^* & 0 \\ 0 & i(\delta + \Delta/2) - \Gamma/2 & 0 & 0 & 0 & -iV_2 & i2V_1 & 0 \\ 0 & 0 & -i(\delta - \Delta/2) - \Gamma/2 & 0 & 0 & iV_1^* & 0 & -i2V_2^* \\ 0 & 0 & 0 & i(\delta - \Delta/2) - \Gamma/2 & -iV_1 & 0 & 0 & i2V_2 \\ iV_2 & 0 & 0 & -iV_1^* & -i\Delta & 0 & 0 & 0 \\ 0 & -iV_2^* & iV_1 & 0 & 0 & i\Delta & 0 & 0 \\ -iV_1 & iV_1^* & -iV_2/2 & iV_2^*/2 & 0 & 0 & -\Gamma/2 & -\Gamma/2 \\ -iV_1/2 & iV_1^*/2 & -iV_2 & iV_2^* & 0 & 0 & -\Gamma/2 & -\Gamma/2 \end{bmatrix} \quad (3.3)$$

The elements of \vec{f} obey the following relations:

$$\langle f_i(t) \rangle = 0, \quad \langle f_i^+(t) f_j(t') \rangle = \langle 2d_{ij} \rangle \delta(t - t') \quad (3.4)$$

where d_{ij} are the elements of the diffusion matrix, \vec{d} . In Appendix A, we show how to calculate this matrix, and how it can be used to find Laplace transforms of two time correlation functions that are needed for the master equation for the probe modes. The magnitude of the damping, Γ , as well as the coefficients thereof in \vec{B} and \vec{C} , can be determined by the usual application of the Wigner–Weisskopf theory of spontaneous emission, incorporating the Lamb shift in the energy difference of the atomic levels, as usual [20].

Using Eqs. (3.4), (3.2) and (3.1), we get the optical Bloch equations:

$$\frac{d}{dt} \langle A_i(t) \rangle = \sum_j B_{ij} \langle A_j(t) \rangle - \frac{\Gamma}{4} (\delta_{i7} + \delta_{i8}) \quad (4.1)$$

The delta correlation of the Langevin force operator implies that we can use the quantum regression theorem, which in turn yields:

$$\frac{d}{dt} \langle A_i(\tau) A_k(0) \rangle = \sum_j B_{ij} \langle A_j(\tau) A_k(0) \rangle - \frac{\Gamma}{4} \langle A_k(0) \rangle (\delta_{i7} + \delta_{i8}) \quad (4.2)$$

The Laplace transform of the two-time correlations is defined as:

$$L_{ij}(s) \equiv \int_0^\infty d\tau e^{-s\tau} A_{ij}(\tau), \quad A_{ij}(\tau) \equiv \langle A_i(\tau) A_j(0) \rangle \quad (5.1)$$

Taking the Laplace transform of Eq. (4.2), we get:

$$sL_{ik}(s) - \sum_j B_{ij} L_{jk}(s) = A_{ik}(0) - \frac{\Gamma}{4s} \langle A_k(0) \rangle (\delta_{i7} + \delta_{i8}) \quad (5.2)$$

In order to solve this algebraic equation for the elements of the matrix $\overline{L}(s)$, we need to find the elements on the right hand side of Eq. (5.2). The vector $\langle A_k(0) \rangle$ corresponds to the steady-state solution of the optical Bloch equations, given by Eq. (4.1). To determine $A_{ik}(0)$, we note that:

$$A_{ik}(0) \equiv \langle A_i(0) A_k(0) \rangle = \left\langle \sum_j \lambda_j A_j(0) \right\rangle = \sum_j \lambda_j \langle A_j(0) \rangle, \quad (5.3)$$

where the coefficients λ_j can be determined by explicit construction, for example.

Table 2
Physical meaning of terms in the master equations

Physical quantity	↔	Terms in master equations
Resonance fluorescence around ω_3	α	$(Q_A + Q_A^*)$
Resonance fluorescence around ω_4	α	$(R_A + R_A^*)$
Gain at ω_3	=	$2\text{Re}(Q_B - Q_A)$
Gain at ω_4	=	$2\text{Re}(R_B - R_A)$
Coupling constant for mixing $\langle a_3 \rangle$ to $\langle a_4^+ \rangle$	=	$-(Q_C - Q_D)$
Coupling constant for mixing $\langle a_4 \rangle$ to $\langle a_3^+ \rangle$	=	$-(R_C - R_D) = (Q_C - Q_D)$

2.3. Master equations for the probe modes

Consider next the interaction of this system with the probe modes. We assume the adiabatic following limit where the atom–pump system equilibrates much faster than the rate of change of probe fields. Under this approximation, we use second order perturbation theory to derive the master equation for the density matrix of the probe modes:

$$\begin{aligned} \dot{\rho} = & \left\{ -Q_A^* a_3 a_3^+ \rho(t) + Q_A a_3^+ \rho(t) a_3 - Q_B a_3^+ a_3 \rho(t) + Q_B^* a_3 \rho(t) a_3^+ \right. \\ & - R_A^* a_4 a_4^+ \rho(t) + R_A a_4^+ \rho(t) a_4 - R_B a_4^+ a_4 \rho(t) + R_B^* a_4 \rho(t) a_4^+ \\ & + Q_C a_3^+ a_4^+ \rho(t) - Q_C^* a_3 \rho(t) a_4 + Q_D^* a_3 a_4 \rho(t) - Q_D a_3^+ \rho(t) a_4^+ \\ & \left. + R_C a_4^+ a_3^+ \rho(t) - R_C^* a_4 \rho(t) a_3 + R_D^* a_4 a_3 \rho(t) - R_D a_4^+ \rho(t) a_3^+ \right\} + \text{adj.} \end{aligned} \tag{6.1}$$

The constant coefficients are weighted elements of the matrix $\overline{L}(s)$ given by

$$\begin{aligned} Q_A^* &= |g_3|^2 L_{12}(-iq), & R_A^* &= |g_4|^2 L_{34}(iq), \\ Q_B &= |g_3|^2 L_{21}(iq), & R_B &= |g_4|^2 L_{43}(-iq), \\ Q_C &= -(g_3^* g_4^*) L_{24}(iq), & R_C &= -(g_3^* g_4^*) L_{42}(-iq), \\ Q_D^* &= -(g_3 g_4) L_{13}(-iq), & R_D^* &= -(g_3 g_4) L_{31}(iq) \end{aligned} \tag{6.2}$$

where q is the frequency difference between the probe and pump modes, defined as

$$q \equiv (\omega_4 - \omega_2) = (\omega_1 - \omega_3) \tag{6.2a}$$

The variables in Eq. (6.2) represent various physical quantities, as shown in Table 2. We will establish the validity of Table 2 throughout the rest of this paper.

2.4. Wave equation for the probe fields

The master equation (Eq. (6.1)) can be used to generate the wave mixing equations for the evolution of the probe modes, by using the relation:

$$\langle \dot{a}_j \rangle = \text{tr}(a_j \dot{\rho}), \quad j = 3,4 \tag{7.1}$$

and the bosonic commutation relations:

$$[a_j, a_k^+] = \delta_{jk}, \quad [a_j, a_k] = 0, \quad j = 3,4; \quad k = 3,4. \tag{7.2}$$

The resulting equation can be expressed as:

$$\langle \dot{\vec{\alpha}} \rangle = -\overline{L} \cdot \langle \vec{\alpha} \rangle \tag{8.1}$$

where

$$\vec{\alpha} \equiv \begin{bmatrix} a_3 \\ a_3^+ \\ a_4 \\ a_4^+ \end{bmatrix}, \quad \overline{L} \equiv \begin{bmatrix} \tilde{\alpha}_3 & 0 & 0 & -\tilde{\chi}_3 \\ 0 & \tilde{\alpha}_3^* & -\tilde{\chi}_3^* & 0 \\ 0 & -\tilde{\chi}_4 & \tilde{\alpha}_4 & 0 \\ -\tilde{\chi}_4^* & 0 & 0 & \tilde{\alpha}_4^* \end{bmatrix} \tag{8.2}$$

with the elements of \bar{A} given by

$$\begin{aligned} \tilde{\alpha}_3 &= Q_B - Q_A, & \tilde{\alpha}_4 &= R_B - R_A \\ \tilde{\chi}_3 &= Q_C - Q_D, & \tilde{\chi}_4 &= R_C - R_D \end{aligned} \tag{8.3}$$

Eq. (8.1) represents the semi-classical wave equation for four-wave mixing in our system. It can also be derived semi-classically using the optical Bloch equations and the Maxwell equations. Here, $-\tilde{\alpha}_j$ represents the complex gain for the field at ω_j , and $-\tilde{\chi}_j$ couples the field at ω_j to the conjugate of the field at ω_k ($j = 3,4; k = 3,4$). When the interaction is sufficiently detuned, the gain terms become much smaller than the mixing terms, leading to nearly ideal four-wave mixing. Note that the phase matching condition for this four-wave mixing process is such that spatially broadband squeezing should occur.

The Langevin equation corresponding to these wave mixing equations can be written as:

$$\dot{\vec{\alpha}} = -\bar{A} \cdot \vec{\alpha} + \vec{F}(t) \tag{8.4}$$

where the elements of the Langevin force obey the following relations:

$$\langle F_i^+(t) \rangle = 0, \quad \langle F_i^+(t) F_j^+(t') \rangle = \langle 2D_{ij} \rangle \delta(t - t') \tag{8.5}$$

with \bar{D} being the diffusion matrix. The elements of \bar{D} will be determined and used later on to determine the spectrum of squeezing in a cavity.

2.5. Equation of motion for the joint photon probability distribution and correlation between the two probe modes

The master equation (Eqs. (6.1), (6.2) and (6.2a)) can be used to generate the equation of motion for the joint photon probability distribution and correlation between the two probe modes. To start with, we denote by $|n\rangle$ and $|m\rangle$ the number states corresponding to the modes at ω_3 and ω_4 , respectively. The general element of the probe fields density matrix can then be written as:

$$P_{nmn'm'} \equiv \langle nm | \rho | n'm' \rangle \tag{9.1}$$

Using the master equation, we then find,

$$\begin{aligned} \dot{P}_{nmn'm'} &= \langle nm | \dot{\rho} | n'm' \rangle \\ &= -Q_A \left[(1+n') P_{nmn'm'} - \sqrt{nn'} P_{(n-1)m(n'-1)m'} \right] - Q_A^* \left[(1+n) P_{nmn'm'} - \sqrt{nn'} P_{(n-1)m(n'-1)m'} \right] \\ &\quad - Q_B \left[n P_{nmn'm'} - \sqrt{(n+1)(n'+1)} P_{(n+1)m(n'+1)m'} \right] \\ &\quad - Q_B^* \left[n' P_{nmn'm'} - \sqrt{(n+1)(n'+1)} P_{(n+1)m(n'+1)m'} \right] \\ &\quad - R_A \left[(1+m') P_{nmn'm'} - \sqrt{mm'} P_{n(m-1)n'(m'-1)} \right] - R_A^* \left[(1+m) P_{nmn'm'} - \sqrt{mm'} P_{n(m-1)n'(m'-1)} \right] \\ &\quad - R_B \left[m P_{nmn'm'} - \sqrt{(m+1)(m'+1)} P_{n(m+1)n'(m'+1)} \right] \\ &\quad - R_B^* \left[m' P_{nmn'm'} - \sqrt{(m+1)(m'+1)} P_{n(m+1)n'(m'+1)} \right] \\ &\quad + Q_C \left[\sqrt{nm} P_{(n-1)(m-1)n'm'} - \sqrt{m(n'+1)} P_{n(m-1)n'(m'+1)} \right] \\ &\quad + Q_C^* \left[\sqrt{n'm'} P_{nm(n'-1)(m'-1)} - \sqrt{m'(n+1)} P_{(n+1)m n'(m'-1)} \right] \\ &\quad + Q_D \left[\sqrt{(n'+1)(m'+1)} P_{nm(n'+1)(m'+1)} - \sqrt{n(m'+1)} P_{(n-1)m n'(m'+1)} \right] \\ &\quad + Q_D^* \left[\sqrt{(n+1)(m+1)} P_{(n+1)(m+1)n'm'} - \sqrt{n'(m+1)} P_{n(m+1)n'(m'+1)} \right] \\ &\quad + R_C \left[\sqrt{mn} P_{(n-1)(m-1)n'm'} - \sqrt{n(m'+1)} P_{(n-1)m n'(m'+1)} \right] \\ &\quad + R_C^* \left[\sqrt{m'n'} P_{nm(n'-1)(m'-1)} - \sqrt{n'(m+1)} P_{n(m+1)n'(m'+1)} \right] \\ &\quad + R_D \left[\sqrt{(m'+1)(n'+1)} P_{nm(n'+1)(m'+1)} - \sqrt{m(n'+1)} P_{n(m-1)n'(m'+1)} \right] \\ &\quad + R_D^* \left[\sqrt{(m+1)(n+1)} P_{(n+1)(m+1)n'm'} - \sqrt{m'(n+1)} P_{(n+1)m n'(m'-1)} \right] \end{aligned} \tag{9.2}$$

This equation can be integrated numerically to determine the exact state of the probe fields. We will use this approach to compute the twin-beam correlation in the four-wave mixing process.

2.6. Phase squeezing in a cavity using the three-level (Λ) system

To start with, we consider a configuration analogous to the experiment of Slusher et al. [1], illustrated schematically in Fig. 2. The forward and backward pump beams are generated by down and up shifting the laser frequency by equal amounts, respectively. The vacuum cavity is servo-locked to the frequencies ω_3 and ω_4 , and encloses the interaction region. Quantum noise builds up in the cavity that, due to the four-wave mixing process, develops correlations between the sidemodes. Squeezing is observed in a linear combination of the sidemodes a_3 and a_4 . To detect the squeezing, a balanced homodyne detection scheme is used wherein the sidemode fields exiting the cavity are mixed with a local oscillator at the laser frequency, ω_L . The phase, ϕ , of the local oscillator is varied by scanning a piezo-mounted mirror. This homodyne detection permits the direct measurement of the variance for any relative phase shift ϕ .

When the noise spectrum of this balanced homodyne detection scheme is observed as a function of this phase, the signal, at the frequency $(\omega_L - \omega_3) = (\omega_4 - \omega_L)$, varies sinusoidally, dipping below the shot noise level for one phase, while rising above the shot noise level for the quadrature phase. If the local oscillator phase is locked to the minimum of these fringes, the observed noise is smaller than the shot-noise, which corresponds to squeezing.

It is easy to show [see Appendix A] that the variance of the squeezed quadrature is given by:

$$V_{\min} = \frac{1}{4} [1 - G(0)] \tag{10.1}$$

$$G(\delta_C) = \gamma_C [2|J_{13}(\delta_C)| - J_{12}(\delta_C) - J_{34}(\delta_C)] \tag{10.2}$$

where γ_C is the cavity decay rate, and $J_{ij}(\delta_C)$ are Fourier components of the two-time correlation functions between the elements of the probe-conjugate state vector $\vec{\alpha}$ in Eq. (8.2):

$$J_{ij}(\delta_C) \equiv \int_{-\infty}^{\infty} \exp(-i\delta_C t) \langle \alpha_i(t) \alpha_j(0) \rangle \tag{10.3}$$

The matrix \mathbf{J} is given by:

$$\bar{J}(\delta_C) = (\bar{\Sigma} + i\delta_C)^{-1} \cdot 2\bar{D} \cdot (\bar{\Sigma}^T - i\delta_C)^{-1} \tag{10.4}$$

where $\bar{\Sigma} = \bar{\Lambda} + \gamma_C/2$ with $\bar{\Lambda}$ given by Eq. (8.2), and \bar{D} being the diffusion matrix in Eq. (8.5).

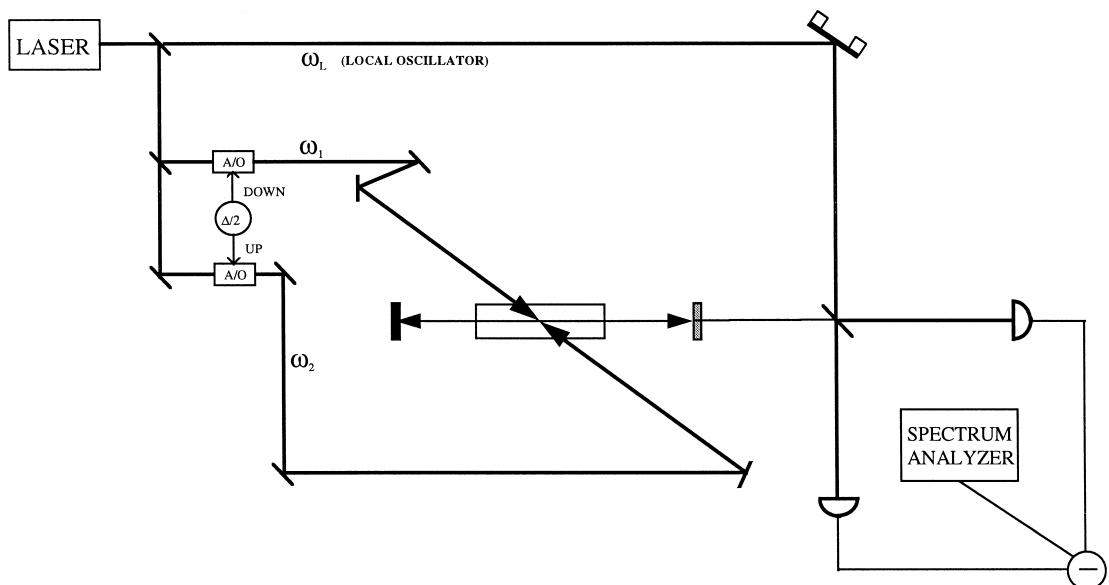


Fig. 2. Schematic illustration of phase squeezing via four-wave mixing in a cavity.

As shown in Appendix A, the elements of this diffusion matrix can be determined from the master equation, and are given by:

$$2\bar{D} = \begin{bmatrix} 0 & (Q_A + Q_A^*) & (Q_C + R_C) & 0 \\ (Q_A + Q_A^*) & 0 & 0 & (Q_C^* + R_C^*) \\ (Q_C + R_C) & 0 & 0 & (R_A + R_A^*) \\ 0 & (Q_C^* + R_C^*) & (R_A + R_A^*) & 0 \end{bmatrix} \quad (11)$$

Fig. 3 shows a typical plot generated from these calculations. Here, we consider the situation where all the beams are plane waves, and the two pumps have equal intensities. F is detuned from resonance by 20Γ , and B is detuned by 60Γ , where Γ is the linewidth of level 2. The cavity decay rate is taken to be 0.02Γ , the cavity volume is 1 cm^3 , and the number of atoms in the cavity is 1.5×10^7 . The horizontal scale is the parameter q shown in Fig. 1, which corresponds to the frequency difference between B and S, which in turn is the same as the frequency difference between C and F. The rabi frequency in each pump is 80Γ ; for ^{87}Rb , this corresponds to about 1 W/mm^2 in each beam, easily accessible from a Ti-Sapphire laser without focusing. As can be seen, much unlike the two-level system, there is significant squeezing (close to 10 dB) even at such modest pump powers. When the pump powers and detunings are scaled, the squeezing also scales. For example, doubling the intensities and detunings increases the squeezing by about 3 dB (i.e., about a factor of 2 on a linear scale).

2.7. Twin beam squeezing in the three-level (Λ) system

For the conditions under which quadrature squeezing occurs, the amplified signal, and conjugate photons are highly correlated. This fact can be used to observe quantum noise suppression more directly. Specifically, if S' and C (in Fig. 1b) are detected with a pair of matched photodiodes connected in reverse, then the net signal represents the subtracted noise from S' and C. For hypothetical conditions of perfect squeezing, there would be zero quantum noise observed. More generally, the correlation between S' and C result in suppression of quantum noise to about the same degree as the quadrature squeezing. This manifestation of noise suppression is called twin beam squeezing. For preliminary experimental observation, this is the easiest approach.

For the condition of best squeezing under the parameters of Fig. 3, we have integrated the equation of motion (Eq. (9.2)) for the joint photon probability distribution and correlation between S' and C, to predict the degree of twin beam squeezing. The sheer size of the matrices (which go as the fourth power of the number of photons that are included) prohibits us from performing this calculation for anything but very weak input signal. Nonetheless, the basic result should be valid for stronger signals as well.

Fig. 4 illustrates the primary results of this calculation. Here the solid curve shows progressive squeezing with increasing product of density and interaction time. As can be seen, the degree of squeezing is approaching the nearly 10 dB squeezing

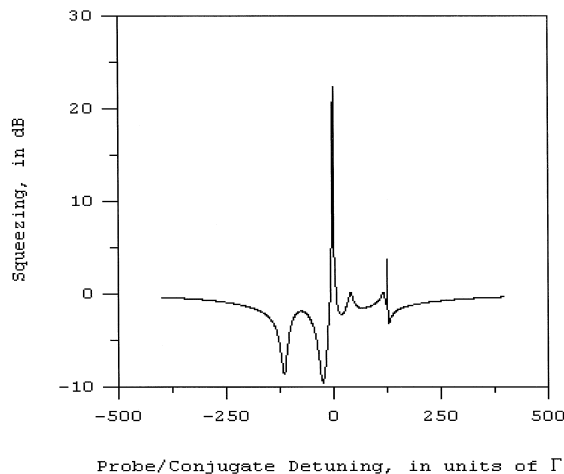


Fig. 3. Theoretical quadrature squeezing, as a function of probe or conjugate detuning.

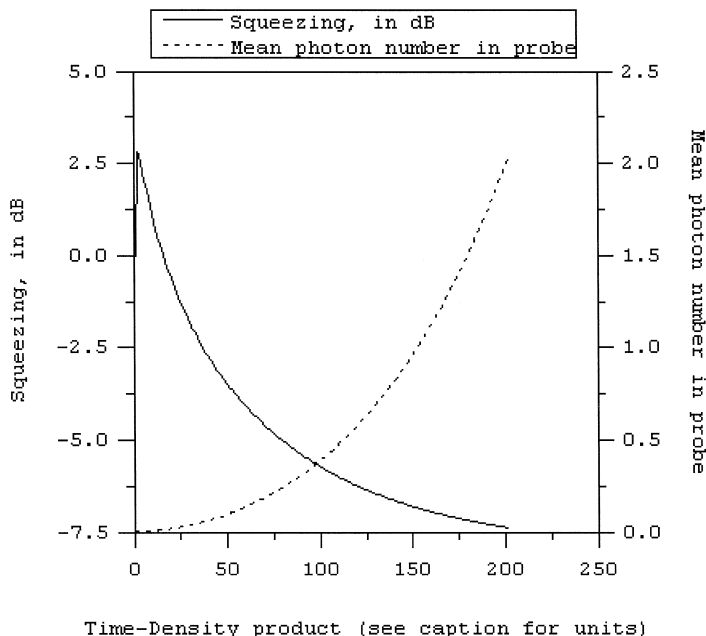


Fig. 4. Progression of twin beam squeezing and mean probe intensity, as a function of the product of interaction time and density (for a density of $1.5 \times 10^7 \text{ cm}^{-3}$, the unit of time is Γ^{-1} , where Γ is the level 2 linewidth).

predicted in Fig. 3. The dotted line shows the amplification of the signal. Fig. 5 shows the comparison between the amplified probe and the conjugate. As can be seen, they are quite well matched.

Fig. 6 illustrates the noise statistics of the amplified probe and conjugate beams. The solid line shows the photon probability distribution of the amplified probe (which in this case exactly matches that of the conjugate) after the interaction

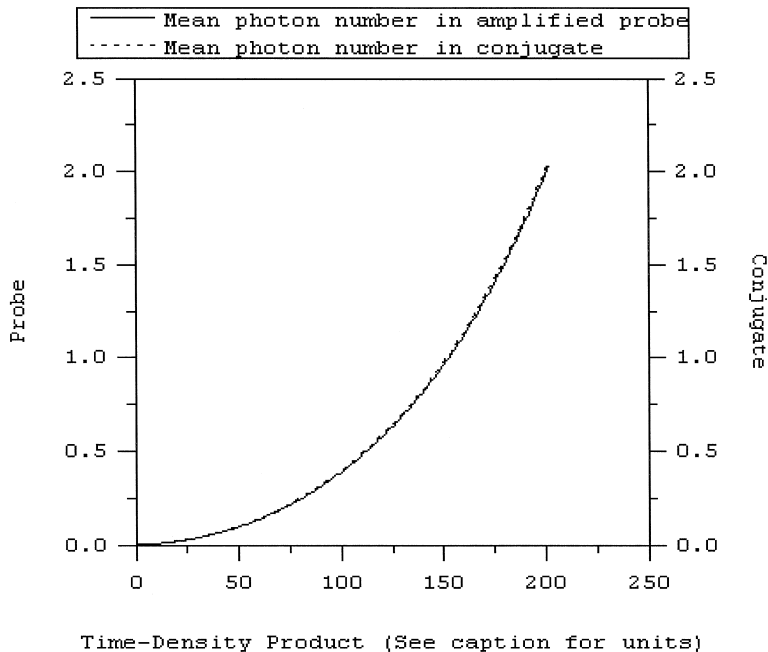


Fig. 5. Progression of mean conjugate and mean probe intensities, as a function of the product of interaction time and density (for a density of $1.5 \times 10^7 \text{ cm}^{-3}$, the unit of time is Γ^{-1} , where Γ is the level 2 linewidth).

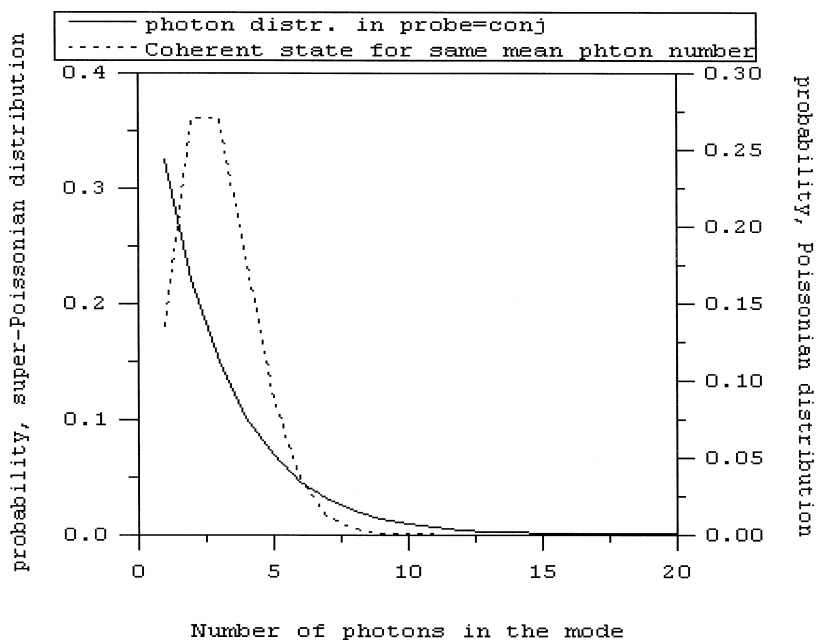


Fig. 6. Comparison of photon distribution of amplified probe with that for a coherent state with the same mean intensity.

has ended. To interpret the statistics of this distribution, we compare this with a coherent state distribution having the same mean photon number. As can be seen, the distribution is not Poissonian, unlike the coherent state. In fact, it has a variance that is larger than that for the corresponding Poissonian distribution. Therefore, the amplified probe and the conjugate are

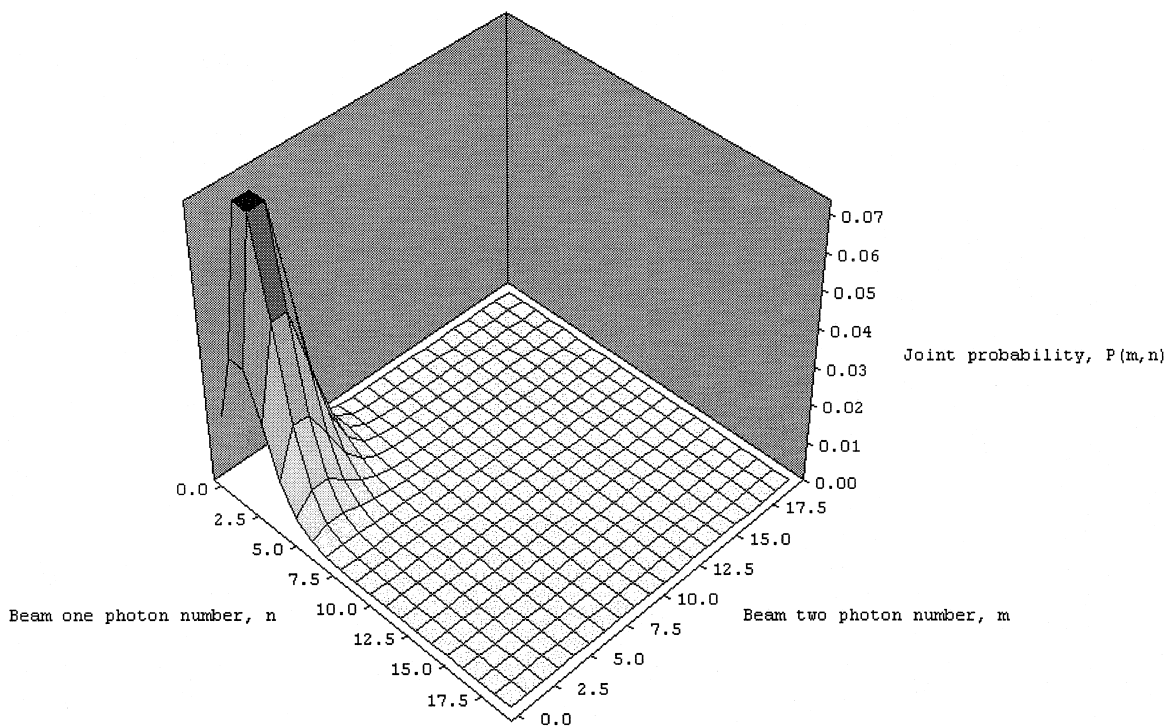


Fig. 7. The joint photon probability distribution for a pair of beams that are each in coherent state (with the same mean intensity as the amplified probe of Fig. 6), but are not twin beams.

each more noisy than coherent light. However, because of the correlation between them, the subtracted noise is much less than that from the coherent state. For the same reason, a linear combination of the amplified probe and the conjugate yield sub-shot-noise measurements at a particular phase, as discussed above.

Note that neither matched photon distribution, nor matched mean intensity mean quantum correlation. For example, two pieces of a laser beam split by a conventional 50/50 beam splitter also have matched photon probability distribution as well as mean intensities. The true picture emerges when one looks directly at the joint photon probability distribution of the two beams. Fig. 7 shows such a distribution for the squeezed twin beams, corresponding to the results shown in Figs. 4 and 5. As can be seen, the joint photon probability distribution of the amplified probe and the conjugate is sharply correlated.

3. Conclusion

We have shown theoretically that non-degenerate four-wave mixing in a Λ system yields strong suppression of quantum phase noise when the probe and conjugate beams are monitored via balanced homodyne detection. Unlike previous calculations performed on similar system, we include situations where the pump beams become resonant with the corresponding two-level transitions. As a result, we find conditions wherein strong squeezing can be achieved with relatively modest pump powers. Furthermore, we show explicitly, via numerical integration, that the probe and the conjugate beams, each starting from the vacuum, are twin beams, containing matching number of photons. The low-power, high gain phase conjugation observed experimentally by us in rubidium vapor under similar conditions indicate the feasibility of realizing a spatially broad band source of squeezed light, with applications to fast detection of faint images, as well as to high-density optical interconnects.

Acknowledgements

We acknowledge helpful discussions with Prof. S. Ezekiel at MIT, and Prof. P. Kumar at Northwestern University. This work was supported in part by AFRL grant no. F30602-97-C-0136.

Appendix A. Two-time correlations and the diffusion matrix

A.1. Basic relations

Here, we review briefly the generalized Einstein relations, how it is used to compute the diffusion matrix for the probe modes, and how the squeezing spectrum is calculated from the elements of the diffusion matrix. In addition, we show how the diffusion matrix for the atom–pump interaction can be obtained.

Consider first a Langevin equation of the form:

$$\dot{\vec{\alpha}}(t) = -\bar{A} \cdot \vec{\alpha}(t) + \vec{F}(t) \tag{A.1}$$

where \bar{A} is an $N \times N$ matrix, and

$$\vec{\alpha}(t) \equiv \begin{bmatrix} \alpha_1 \\ \alpha_2 \\ \vdots \\ \alpha_N \end{bmatrix}, \quad \vec{F}(t) \equiv \begin{bmatrix} F_1 \\ F_2 \\ \vdots \\ F_N \end{bmatrix}, \quad \begin{aligned} \langle F_j(t) \rangle &= 0 \\ \langle F_i^+(t) F_j(t') \rangle &= 2\bar{D}_{ij} \delta(t-t') \end{aligned} \tag{A.2}$$

with \bar{D} being the diffusion matrix. Given the properties of the Langevin force, \vec{F} , we can write the generalized Einstein relation in the form:

$$\frac{\partial}{\partial t} \langle \vec{\alpha}(t) \vec{\alpha}^T(t) \rangle = \langle \vec{\beta}(t) \vec{\alpha}^T(t) \rangle + \langle \vec{\alpha}(t) \vec{\beta}^T(t) \rangle + 2\bar{D} \tag{A.3}$$

where $\vec{\beta}(t) \equiv -\bar{A} \cdot \vec{\alpha}(t)$ is the drift matrix. Here, we have, for example, defined $\vec{\alpha}(t) \vec{\alpha}^T(t)$, an $N \times N$ matrix, as the outer product of the form:

$$\vec{\alpha}(t) \vec{\alpha}^T(t) \equiv \begin{bmatrix} \alpha_1 \\ \alpha_2 \\ \vdots \\ \alpha_N \end{bmatrix} \otimes [\alpha_1 \ \alpha_2 \ \dots \ \alpha_N] \tag{A.4}$$

In algebraic form, the Einstein relation can be rewritten as:

$$2D_{ij} = -\langle \beta_i(t) \alpha_j(t) \rangle - \langle \alpha_i(t) \beta_j(t) \rangle + \frac{\partial}{\partial t} \langle \alpha_i(t) \alpha_j(t) \rangle \tag{A.5}$$

In steady-state, we can set $t = 0$, and find:

$$2\bar{D} = -\langle \vec{\beta}(0) \vec{\alpha}^T(0) \rangle - \langle \vec{\alpha}(0) \vec{\beta}^T(0) \rangle = \bar{\Lambda} \langle \vec{\alpha}(0) \vec{\alpha}^T(0) \rangle + \langle \vec{\alpha}(0) \vec{\alpha}^T(0) \rangle \bar{\Lambda}^T \tag{A.6}$$

This relation can be used to determine the diffusion matrix, since the expectation value of $\langle \vec{\alpha}(0) \vec{\alpha}^T(0) \rangle$ can be determined from the value $\langle \vec{\alpha}(0) \rangle$, found by solving the mean-value equation

$$\dot{\langle \vec{\alpha}(t) \rangle} = -\bar{\Lambda} \cdot \langle \vec{\alpha}(t) \rangle \tag{A.7}$$

in steady-state. Alternatively, one can use Eq. (A.5) to find the diffusion matrix.

The diffusion matrix can be used to determine the spectrum of two-time correlation functions. To show this, we first use the quantum regression theorem (which follows from the properties of the Langevin force elements) to derive the equation of motion of the two time correlation functions:

$$\frac{\partial}{\partial \tau} \langle \vec{\alpha}(\tau) \vec{\alpha}^T(0) \rangle = -\bar{\Lambda} \cdot \langle \vec{\alpha}(\tau) \vec{\alpha}^T(0) \rangle \tag{A.8}$$

The formal solution of this equation can be written as:

$$\langle \vec{\alpha}(\tau) \vec{\alpha}^T(0) \rangle = \exp(-\bar{\Lambda}\tau) \cdot \langle \vec{\alpha}(0) \vec{\alpha}^T(0) \rangle \tag{A.9}$$

Similarly, we can write:

$$\langle \vec{\alpha}(0) \vec{\alpha}^T(\tau) \rangle = \langle \vec{\alpha}(0) \vec{\alpha}^T(0) \rangle \cdot \exp(-\bar{\Lambda}^T\tau). \tag{A.10}$$

Consider next the Fourier transform of the two-time correlation functions:

$$\begin{aligned} \bar{J}(\varepsilon) &\equiv \int_{-\infty}^{\infty} d\tau \exp(-i\varepsilon\tau) \langle \vec{\alpha}(\tau) \vec{\alpha}^T(0) \rangle \\ &= \int_0^{\infty} d\tau \exp(-i\varepsilon\tau) \langle \vec{\alpha}(\tau) \vec{\alpha}^T(0) \rangle + \int_{-\infty}^0 d\tau \exp(-i\varepsilon\tau) \langle \vec{\alpha}(0) \vec{\alpha}^T(-\tau) \rangle \\ &= \int_0^{\infty} d\tau \exp(-i\varepsilon\tau) \langle \vec{\alpha}(\tau) \vec{\alpha}^T(0) \rangle + \int_0^{\infty} d\tau \exp(i\varepsilon\tau) \langle \vec{\alpha}(0) \vec{\alpha}^T(\tau) \rangle \end{aligned} \tag{A.11}$$

Using Eqs. (A.9) and (A.10), we get:

$$\bar{J}(\varepsilon) = (\bar{\Lambda} + i\varepsilon)^{-1} \cdot \langle \vec{\alpha}(0) \vec{\alpha}^T(0) \rangle + \langle \vec{\alpha}(0) \vec{\alpha}^T(0) \rangle \cdot (\bar{\Lambda}^T - i\varepsilon)^{-1} \tag{A.12}$$

Using Eqs. (A.6) and (A.12), after simple algebra, we get:

$$\bar{J}(\varepsilon) = (\bar{\Lambda} + i\varepsilon)^{-1} \cdot 2\bar{D} \cdot (\bar{\Lambda}^T - i\varepsilon)^{-1} \tag{A.13}$$

A.2. Application to atom–pump interaction

The Langevin equation describing the atom–pump interaction has the inhomogeneous form given by:

$$\dot{\vec{A}}(t) = \bar{B} \cdot \vec{A}(t) + \vec{C} + \vec{f}(t) \tag{A.14}$$

To turn this into a homogeneous equation, we define:

$$\vec{K} \equiv \bar{B}^{-1} \vec{C}, \quad \vec{a}(t) \equiv \vec{A}(t) + \vec{K} \tag{A.15}$$

which yields:

$$\dot{\vec{a}}(t) = \bar{B} \cdot \vec{a}(t) + \vec{f}(t) \tag{A.16}$$

From the relations derived above, we then find the diffusion matrix as:

$$2\bar{d} = -\bar{B}\langle\bar{a}(0)\bar{a}^T(0)\rangle - \langle\bar{a}(0)\bar{a}^T(0)\rangle\bar{B}^T \quad (\text{A.17})$$

We determine \bar{d} by using Eq. (A.15) and the steady-state solution of the optical Bloch equations. The Fourier transforms of the two time correlation functions can then be determined by using Eq. (A.13).

A.3. Application to the squeezing spectrum outside a cavity

Inside the cavity, the Langevin equation describing the evolution of the probe modes can be written as:

$$\dot{\bar{\alpha}}(t) = -\bar{\Sigma} \cdot \bar{\alpha}(t) + \bar{F}(t) \quad (\text{A.18})$$

where $\bar{\Sigma} = \bar{\Lambda} + \gamma_C/2$, with $\bar{\Lambda}$ given by Eq. (8.2), and γ_C being the cavity decay rate. From this equation, we can use the expression in Eq. (A.6) to find the diffusion matrix, \bar{D} as shown in Eq. (11). The master equation is used to find the third term on the right-hand side of Eq. (A.6):

$$\frac{\partial}{\partial t} \langle \alpha_i(t) \alpha_j(t) \rangle = \langle \dot{\rho}(t) \alpha_i(t) \alpha_j(t) \rangle \quad (\text{A.19})$$

The spectrum matrix, $\bar{J}(\varepsilon)$, is then given by Eq. (A.13):

$$\bar{J}(\varepsilon) = (\bar{\Sigma} + i\varepsilon)^{-1} \cdot 2\bar{D} \cdot (\bar{\Sigma}^T - i\varepsilon)^{-1} \quad (\text{A.20})$$

References

- [1] R.E. Slusher, L.W. Hollberg, B. Yurke, J.C. Mertz, J.F. Valley, Phys. Rev. Lett. 55 (1985) 2409.
- [2] A. Aytur, P. Kumar, Phys. Rev. Lett. 65 (1990) 1551.
- [3] L. Wu, H.J. Kimble, J.L. Hall, H. Wu, Phys. Rev. Lett. 57 (1986) 2520.
- [4] C.M. Caves, Phys. Rev. D 26 (1982) 1817.
- [5] C.W. Misner, K.S. Thorne, J.A. Wheeler, Gravitation, Freeman, San Francisco, 1973.
- [6] M. Xiao, L. Wu, H.J. Kimble, Phys. Rev. Lett. 59 (1987) 278.
- [7] T.A. Dorschner, H.A. Haus, M. Holz, I.W. Smith, H. Statz, IEEE J. Quantum Electron. 16 (1980) 1376.
- [8] M.I. Kolobov, P. Kumar, Opt. Lett. 18 (1993) 849.
- [9] B.S. Ham, M.S. Shahriar, M.K. Kim, P.R. Hemmer, Opt. Lett. 22 (1997) 1849.
- [10] B. Kohler, S. Burnet, A. Renn, U.P. Wild, Opt. Lett. 18 (1993) 2144.
- [11] T. Mosberg, personal communication.
- [12] H.P. Yuen, J.H. Shapiro, Opt. Lett. 4 (1979) 334.
- [13] M. Valet, M. Pinard, G. Grynberg, Opt. Commun. 81 (1991) 403.
- [14] G. Alzetta, A. Gozzini, L. Moi, G. Orriols, Nuovo Cimento B 36 (1976) 5.
- [15] H.R. Gray, R.M. Whitley, C.R. Stroud, Opt. Lett. 3 (1978) 218.
- [16] T.T. Grove, E. Rousseau, X.-W. Xia, D.S. Hsuing, M.S. Shahriar, P.R. Hemmer, Opt. Lett. 22 (1997) 1677.
- [17] P.R. Hemmer, D.P. Katz, J. Donoghue, M. Cronin-Golomb, M.S. Shahriar, P. Kumar, Opt. Lett. 20 (1995) 982.
- [18] T.T. Grove, M.S. Shahriar, P.R. Hemmer, P. Kumar, V.K. Sudarshanam, M. Cronin-Golomb, Opt. Lett. 22 (1997) 769.
- [19] M.D. Reid, D.F. Walls, B.J. Dalton, Phys. Rev. Lett. 55 (1985) 1288.
- [20] M.S.K. Razmi, J.H. Eberly, Opt. Commun. 76 (1990) 265.
- [21] N.N. Bogolubov Jr., A.S. Shumovsky, T. Quang, J. Phys. B 20 (1987) L447.
- [22] D. Holm, M. Sargent III, Phys. Rev. A 35 (1987) 2150.